

Article (refereed) - postprint

Tramblay, Yves; Rutkowska, Agnieszka; Sauquet, Eric; Sefton, Catherine; Laaha, Gregor; Osuch, Marzena; Albuquerque, Teresa; Alves, Maria Helena; Banasik, Kazimierz; Beaufort, Aurelien; Brocca, Luca; Camici, Stefania; Csabai, Zoltán; Dakhlaoui, Hamouda; DeGirolamo, Anna Maria; Dörflinger, Gerald; Gallart, Francesc; Gauster, Tobias; Hanich, Lahoucine; Kohnová, Silvia; Mediero, Luis; Plamen, Ninov; Parry, Simon; Quintana-Seguí, Pere; Tzoraki, Ourania; Datry, Thibault. 2021. **Trends in flow intermittence for European rivers.** *Hydrological Sciences Journal*, 66 (1). 37-49.

© 2020 IAHS

This version is available at <http://nora.nerc.ac.uk/id/eprint/529163>

Copyright and other rights for material on this site are retained by the rights owners. Users should read the terms and conditions of use of this material at <https://nora.nerc.ac.uk/policies.html#access>

This is an Accepted Manuscript of an article published by Taylor & Francis in *Hydrological Sciences Journal* on January 2021, available online: <https://doi.org/10.1080/02626667.2020.1849708>.

There may be differences between the Accepted Manuscript and the final publisher's version. You are advised to consult the publisher's version if you wish to cite from this article.

The definitive version is available at <https://www.tandfonline.com>

Contact UKCEH NORA team at
noraceh@ceh.ac.uk

1 **Trends in flow intermittence for European Rivers**

- 2
- 3 Trambly Yves (HydroSciences Montpellier, Univ. Montpellier, CNRS, IRD, France) *
- 4 Rutkowska Agnieszka (University of Agriculture in Kraków, Poland)
- 5 Sauquet Eric (INRAE, France)
- 6 Sefton Catherine (UKCEH, UK)
- 7 Lahaa Gregor (BOKU, Austria)
- 8 Osuch Marzena (Institute of Geophysics, Polish Academy of Sciences, Poland)
- 9 Albuquerque Teresa (IPCB|Cernas|QRural and ICT|University of Évora, Portugal)
- 10 Alves Maria Helena (Portuguese Environment Agency, Lisbon, Portugal)
- 11 Banasik Kazimierz (Warsaw University of Life Sciences - SGGW, Poland)
- 12 Beaufort Aurelien (INRAE, France)
- 13 Brocca Luca (IRPI-CNR, Italy)
- 14 Camici Stefania (IRPI-CNR, Italy)
- 15 Csabai Zoltán (Department of Hydrobiology, University of Pécs, Hungary and Department of Botany and Zoology,
16 Masaryk University, Brno, Czech Republic)
- 17 Dakhlaoui Hamouda (ENIT, Tunisia)
- 18 DeGirolamo Anna Maria (IRSA-CNR, Italy)
- 19 Dörflinger Gerald (Water Development Department, Cyprus)
- 20 Gallart Francesc (IDAEA, CSIC, Spain)
- 21 Gauster Tobias (Boku, Austria)
- 22 Hanich Lahoucine (L3G Laboratory, Earth Sciences Department, Faculty of Sciences & Techniques, Cadi Ayyad
23 University, BP 459, 40000 Marrakech, Morocco, and Mohammed VI Polytechnic University (UM6P), Morocco,
24 Centre for Remote Sensing and Application)
- 25 Kohnová Silvia (Slovak University of Technology, Faculty of Civil Engineering, Department of Land and Water
26 Resources Management, Slovakia)
- 27 Mediero Luis (UPM, Spain)
- 28 Ninov Plamen (Bulgarian Academy of Sciences, Sofia, Bulgaria)
- 29 Parry Simon (UKCEH, UK)
- 30 Quintana-Seguí Pere (Observatori de l'Ebre, Universitat Ramon Llull – CSIC, Roquetes, Spain)
- 31 Tzoraki Ourania (University of the Aegean, Greece)
- 32 Datry Thibault (INRAE, France)

33

34 *Corresponding author: yves.trambly@ird.fr

35

36 Revised manuscript v3, 10/09/2020

37 **Abstract**

38

39 Intermittent rivers are prevalent in many countries across Europe, but little is known about the
40 temporal evolution of intermittence and their relationships with climate variability. In this study, a
41 trend analysis is performed on the annual and seasonal number of zero-flow days, the maximum
42 duration of dry spells and the mean date of the zero-flow events, on a database of 452 rivers with
43 varying degrees of intermittence between 1970 and 2010. In addition, the relationships between
44 flow intermittence and climate are investigated using the Standardized Precipitation
45 Evapotranspiration Index (SPEI) and climate indices describing large scale atmospheric
46 circulation. Results indicated a strong spatial variability of the seasonal patterns of intermittence
47 and the annual and seasonal number of zero-flow days, which highlights the controls exerted by
48 local catchment properties. Most of the detected trends indicate an increasing number of zero-flow
49 days which also tend to occur earlier in the year, in particular in Southern Europe. The SPEI is
50 found to be strongly related to the annual and seasonal zero-flow day occurrence in more than half
51 of the stations for different accumulation times between 12 and 24 months. Conversely, there is a
52 weaker dependence of river intermittence with large-scale circulation indices. Overall, these results
53 suggest increased water stress in intermittent rivers that may affect their biota and biochemistry
54 and also reduce available water resources.

55

56

57

58

59

60 **Keywords:** Europe, Intermittent, Ephemeral, Rivers, Trends, SPEI, seasonality, zero-flows

61

62

63

64

65

66

67

68 1. INTRODUCTION

69
70 In streams and rivers, flow intermittence is characterized by the cessation of flow, followed or not
71 by complete drying of the channels (Datry et al. 2017). The spatio-temporal patterns of flow
72 intermittence can be extremely variable depending on climatic, geologic or topographic contexts
73 (Costigan et al. 2017). While many studies have been focused on river low-flows characterization
74 and, in particular, the possible long-term trends due to climate change (e.g., Marx et al., 2018), far
75 less work has been dedicated to intermittent rivers and ephemeral streams. Recent studies indicate
76 trends towards less severe climatic droughts over North-Eastern Europe, especially in winter and
77 spring, and the opposite in Southern Europe where more severe droughts, are encountered (Spinoni
78 et al., 2017, Hertig and Trambly, 2017). Globally, negative trends in streamflow in Europe have
79 been reported by Stahl et al. (2010), in Spain by Gallart and Llorens (2004), Coch and Mediero
80 (2016), in Italy by De Girolamo et al. (2017), Germany by Bormann and Pinter (2017) and in
81 Cyprus by Myronidis et al. (2018).

82
83 To our knowledge, no studies have explored the trends in flow intermittence across Europe. Snelder
84 et al. (2013) analyzed French patterns in flow intermittence, using as indicators the mean annual
85 frequency of zero-flow periods and the mean duration of zero-flow periods. Unsurprisingly, the
86 highest values of the two characteristics coincided with the years of severe droughts. Besides
87 climate influences, intermittence characteristics might be strongly influenced by processes
88 operating at small scales, including groundwater-surface water interactions, river transmission
89 losses, frozen surface water, flow reversal, instrument error, natural or human-driven discharge
90 losses (Beaufort et al., 2019, Costigan et al. 2017, Zimmer et al., 2020). Similarly, in different
91 regions of the USA, Eng et al. (2016) classified 265 intermittent streams using as descriptors the
92 number of zero-flow events, the median discharge and the 10th percentile of daily flows, and they
93 showed the strong dependency of these metrics with temporal variations of precipitation and
94 evapotranspiration. More generally, the probability of flow intermittence in rivers worldwide is
95 likely to increase with the projected rise of temperature in future climate scenarios (Döll & Schmied
96 2012, Osuch et al., 2018, Snelder et al. 2013, Eng et al. 2016).

97

98 Previous classifications of European rivers based on their flow regime have usually not integrated
99 flow intermittence or in a relatively small sample of basins (Gallart et al., 2010, Oueslati et al.,
100 2015). This is probably due to the difficulties in conceptually defining the intermittent, ephemeral
101 and perennial aquatic states of streams (Gustard et al., 1992, Oueslati et al., 2015, Delso et al.,
102 2017). For low flows and hydrological droughts, regional classifications at the European scale (e.g.
103 Stahl and Demuth, 1999, Hannaford et al., 2011, Kirkby et al., 2011) or national scale (in Spain,
104 Coch and Mediero, 2016) have been produced using most often the flow exceeded 90% of the time
105 as a threshold for low flows. Only a few classifications of intermittent rivers based on zero-flow
106 indicators have been proposed, in an attempt to relate their spatiotemporal variability with
107 catchment characteristics or climatic variability (Kennard et al., 2010, Snelder et al., 2013, Eng et
108 al., 2016, Perez-Saez et al., 2017, Tzoraki et al., 2016, Dörflinger, 2016, D'Ambrosio et al., 2017,
109 Pournasiri Poshtiri et al., 2019). Identifying homogeneous regions and the drivers of flow
110 intermittence, in terms of seasonality, catchment or climatic properties, could help to estimate
111 intermittence characteristics and trends at the regional level (Pournasiri Poshtiri et al., 2019).
112 Indeed, these intermittent and ephemeral streams are underrepresented in monitoring networks and
113 often ungauged in Europe (Skoulikidis et al., 2017, Costigan et al., 2017).

114
115 Besides catchment characteristics, large scale climate variability may also exert an influence on
116 intermittence patterns. Giuntoli et al. (2013) evaluated the relationships between low flows and
117 large-scale climate variability in France, using climate indices such as the North Atlantic
118 Oscillation (NAO), the Atlantic Multi-decadal Oscillation (AMO) and a weather typing approach.
119 Their results indicated an increase of drought severity in Southern France, and the usefulness of
120 lagged climate indices as predictors of summer low flows. Indeed, approaches based on weather
121 typing or composite analysis with climatic data could help to evaluate the synoptic ingredients
122 associated with dry periods and their long-term evolution and trends (Stahl and Demuth, 1999,
123 Ionita et al., 2017). For the summer 2015 drought episode that hit large parts of Europe, Ionita et
124 al. (2017) observed that this event was associated with positive anomalies in 500 hPa geopotential
125 height and Mediterranean Sea surface temperatures. Since these climatic drivers are likely to have
126 different influences in different regions of Europe, there is a need to perform such analysis at the
127 regional scale.

128

129 The objectives of this study are: (i) to analyze the seasonal characteristics of flow intermittence in
130 Europe, (ii) to test temporal trends in the number of zero-flow days at annual and seasonal scale
131 and (iii) to analyze the possible relationships between the occurrence of zero-flows and climate
132 indices. This study relies on an unprecedented database of intermittent rivers across Europe, which
133 is presented in the next section, the methodology is presented in section three and the results in
134 section four.

135

136 2. DATABASE OF INTERMITTENT RIVERS

137

138 The database of discharge time series of ephemeral and intermittent streams have been collected in
139 the framework of the SMIRES COST action (Datry et al., 2017) in the different European countries
140 in addition to individual contributions and stations from the GRDC (<https://www.bafg.de/GRDC>)
141 database including countries outside of Europe such as Morocco, Tunisia and Israel. The selected
142 rivers are characterized by natural or moderately influenced flow regime with catchment area
143 smaller than 2000km² (Figure 1). The absence of dams or reservoirs upstream of the station gauge
144 has been verified from a GIS analysis using the GRanD database
145 (<http://globaldamwatch.org/grand/>). It must be noted that the metadata originating from different
146 countries should be analyzed with care and can be misleading since the definition of “natural”, and
147 the distinction between “little influenced” and “heavily” influenced rivers may vary strongly
148 between different countries. Also, since this study is focusing on zero-flow days, it is possible that
149 zero values are put in place of missing data; this is the reason why the data had to be checked
150 carefully in the absence of metadata for many rivers. In cases where the catchment area for a station
151 was missing, the catchment has been delineated using the flow accumulation maps from the
152 HydroSheds database (<https://www.hydrosheds.org/>).

153

154 Instead of using zeros, a threshold of $10^{-4} \text{ m}^3 \cdot \text{s}^{-1}$ ($0.1 \text{ L} \cdot \text{s}^{-1}$) is considered to identify days with river
155 discharge equal to zero, to account for measurements errors of very small discharge values.
156 However other thresholds, such as $5 \text{ L} \cdot \text{s}^{-1}$ recommended by Gustard et al. (1992) or Delso et al.
157 (2017) have also been tested, yielding similar results. In addition to this threshold, the individual
158 time series have been checked to verify if the smallest reported daily discharge values were below
159 $10 \text{ L} \cdot \text{s}^{-1}$. If there were no daily discharge values below $10 \text{ L} \cdot \text{s}^{-1}$ in a series that contained zero-flow

160 days, the zero-flow days of that series were interpreted as wrongly reported missing values and the
161 gage was removed. The analyses performed in the present work are focusing on the annual and
162 seasonal timescales, with the hydrological year starting April 1 through March 31 since this is
163 common practice in low-flow analysis (Laha and Blöschl, 2006). We consider an extended
164 summer season, from April to September, and an extended winter season from October to March.
165 The definition of the hydrological years was governed by a preliminary analysis on the seasonality
166 of zero-flow events in Europe (mainly in summer and fall but also in winter). This reduces the
167 chance of observing a zero-flow event spanning across two consecutive hydrological years. The
168 database includes 452 stations with at least two years with five consecutive zero-flow days. This
169 criterion has been chosen to avoid including in the database some missing data in place of actual
170 river intermittence since it is unlikely that river flow will cease only one day in one year. Indeed,
171 if for an annual time series only a single day with zero-flow is recorded, it could be missing data
172 not properly reported in the metadata. For all stations, all years with more than 5% missing data
173 have been removed. Across most stations (452), there is a common period for analysis between
174 1970 and 2010 when data are available (Figure 1). Two annual and seasonal metrics of duration
175 are considered:(i) the duration of the longest no-flow event (maximum length of zero-flow days)
176 and (ii) the total duration of no-flow days (sum of zero-flow days). The mean date of no-flow days
177 is also considered in the trend analysis..

178

179 **3. METHODS**

180

181 **3.1 Clustering of stations based on seasonality measures**

182

183 Directional statistics can be used to define similarity measures from the timing of zero-flow
184 conditions. The first step is to convert dates into the day-in-year, which is the day of a year starting
185 from 1 April, into an angular value (Burn, 1997):

186

$$187 \theta_i = (\text{Julian Date})_i \left(\frac{2\pi}{365} \right) \quad (1)$$

188

189 where θ_i is the angular value in radians for the zero-flow day I In leap years, the denominator was
190 increased by one. The conversion of Julian days into angular values is convenient to avoid artificial

191 breaks between the last day of the year and the first day of the next year. All zero-flow days can
192 then be seen as vectors with unit magnitude and direction given by θ_i . Then, for a sample of n dates,
193 the \bar{x} and \bar{y} coordinates of the mean date can be determined as:

194
195
$$\bar{x} = \frac{1}{n} \sum_{i=1}^n \cos(\theta_i) \quad (2)$$

196
197
$$\bar{y} = \frac{1}{n} \sum_{i=1}^n \sin(\theta_i) \quad (3)$$

198
199 The mean direction (the mean date) $\bar{\theta} \in [0, 2\pi)$ of zero-flow dates for a given station can be then
200 obtained from:

201
202
$$\bar{\theta} = \arctan^* \left(\frac{\bar{y}}{\bar{x}} \right) \quad (4)$$

203
204 where $\arctan^*(\cdot)$ is the quadrant-specific inverse of the tangent function. The measure of the
205 variability of the n occurrences around the mean date is the mean resultant length:

206
207
$$r = \sqrt{\bar{x}^2 + \bar{y}^2} \quad (5)$$

208
209 It should be noted that $0 < r \leq 1$ and that r near to 1 implies little variation and high concentration
210 of data, and \bar{r} near to 0 a large variation and wide dispersion around the mean date.

211
212 The clustering is based on the matrix including the $\bar{\theta}$ and r metrics calculated for winter and
213 summer for each station. Then a Euclidean distance between stations has been computed and the
214 Ward method (Ward, 1963) has been chosen as the linkage criterion to create clusters. The
215 identification of the optimal number of clusters is achieved with the help of the silhouette plot and
216 visual inspection of the clusters obtained.

217
218 **3.2 Trend analysis**

219

220 Trend analysis has been performed using the modified Mann-Kendall (MK) test (Mann, 1945,
 221 Hamed and Rao, 1998) on the annual and seasonal metrics of duration and occurrence and the mean
 222 date of occurrence $\bar{\theta}$. The MK rank correlation test for two sets of observations $X = x_1, x_2, \dots, x_n$ and
 223 $Y = y_1, y_2, \dots, y_n$ is formulated as follows, with the S statistic calculated as:

$$225 \quad S = \sum_{i < j} a_{ij} b_{ij} \quad (6)$$

226
 227 where

$$229 \quad a_{ij} = \text{sgn}(x_j - x_i) = \begin{cases} 1, & \text{if } x_i < x_j \\ 0, & \text{if } x_i = x_j \\ -1, & \text{if } x_i > x_j \end{cases} \quad (7)$$

230
 231 and b_{ij} is similarly defined for the observations in Y . Under the null hypothesis that X and Y are
 232 independent and randomly ordered, the statistic S tends to normality for large n . In the current
 233 work, the modified MK test proposed by Hamed and Rao (1998) is considered, that is robust in the
 234 presence of autocorrelation in the time series tested by modifying the variance of the S statistic.
 235 The slope of the trends is computed with the Sen slope method.

236
 237 In addition, to consider the issue of false positives due to repeated statistical tests (Wilks, 2016),
 238 the False Discovery Rate (FDR) procedure introduced by Benjamini and Hochberg (1995) has been
 239 implemented to identify field-significant test results. With this method, the results are considered
 240 field significant (or regionally significant) if at least one local p-value of the test is below the global
 241 significance level. Only 254 of the 452 selected stations, those with at least 10 years with more
 242 than five consecutive zero-flow days, have been considered for this analysis to avoid testing trends
 243 on very small sample size. The 10% significance level (p-value =0.1) was considered for trend
 244 detection, in order to avoid discarding weak trends that might be relevant in a changing
 245 environment.

246
 247 **3.3 Relationships with climate**

249 To estimate the relationships between dry spells and climatic drivers, namely precipitation and
250 evapotranspiration, the correlation between the annual and seasonal sum of zero-flow days and the
251 maximum length of zero-flow days with the Standardized Precipitation-Evapotranspiration Index
252 (SPEI, Vicente-Serrano et al., 2010) was analyzed with the Spearman correlation coefficient (ρ).
253 The SPEI uses the monthly difference between precipitation and potential evapotranspiration; thus
254 it represents a simple climatic water balance, which can be calculated at different time scales
255 similarly to the Standardized Precipitation Index (SPI, McKee et al., 1993). The SPEI with 6, 12,
256 18 and 24 months aggregation time have been downloaded from the CSIC Global SPEI database
257 (<https://spei.csic.es/database.html>). The SPEI values from the CSIC database were computed using
258 the monthly sum of precipitation and potential evapotranspiration at 0.5 degrees spatial resolution
259 and a monthly time resolution from the Climatic Research Unit (CRU) of the University of East
260 Anglia. Version 3.23 of the CRU dataset has been used to compute the SPEI. The SPEI computation
261 is based on the FAO-56 Penman-Monteith estimation of potential evapotranspiration. The details
262 of the SPEI computation were presented by Beguería et al. (2014). For each station, the value was
263 extracted from the SPEI grid cell covering the station, since the size of the basins considered is
264 small ($<2000\text{km}^2$) compared to the CRU mesh (approximately 2500km^2) used as a basis for the
265 calculation of the SPEI.

266
267 In addition, different climate indices describing large scale atmospheric circulation patterns have
268 been selected: the North Atlantic Oscillation (NAO), the Atlantic Multi-decadal Oscillation
269 (AMO), the Mediterranean Index (MOI), the East Atlantic Western Russia (EAWR), the Pacific
270 Decadal Oscillation (PDO), and the Scandinavian Index (SCAND). The time series for these
271 indices have been retrieved from the Climate Prediction Center database available online at:
272 <https://www.cpc.ncep.noaa.gov>. The annual, winter and summer mean values were used according
273 to the definition of hydrological year and seasons previously adopted. For NAO, the seasonal three-
274 month DJF, MAM, JJA, and SON values were also included to account for its within-year
275 variability.

276

277 **4. RESULTS**

278

279 **4.1 Seasonal spatiotemporal patterns**

280
281 For 186 stations out of 452 (41%), there is more than 10% mean annual zero-flow days (Figure 2).
282 As shown on the map (Figure 2), the annual percentage of years with zero-flow days can vary
283 strongly even for neighbouring stations. This highlights the influence of local characteristics
284 (geology, land cover, water use...) on zero-flow occurrences. The size of the river is an additional
285 likely explanation for spatially nearby differences in intermittence, with small tributaries flowing
286 into a larger river being more prone to drying. However, there is no clear dependency between the
287 frequency of zero-flow and catchment size, showing that other catchment characteristics, that are
288 not analyzed in the present study, may have a stronger influence on the occurrence of zero-flow
289 days. There is a weak latitudinal gradient in the occurrence of zero-flow days, with the higher mean
290 annual number of zero-flow days in the South ($\rho = -0.36$ with latitude, significant at the 5% level),
291 but with a very strong spatial variability even for neighbouring catchments. This implies that most
292 intermittent streams are not necessarily associated with the most arid climate conditions in
293 Southern Europe. It must be also noted that this observation strongly depends on the density of
294 monitoring networks and their representation of intermittent and ephemeral streams.

295
296 Clustering has been applied using the variables $\bar{\theta}$, the mean direction of zero-flow and the
297 variability around this date, r , computed for the winter and summer seasons. Three different
298 seasonality patterns can be identified in Figure 3. The largest one, the summer cluster, is composed
299 of 376 stations having a mean date of occurrence for zero-flow days between May and November
300 (Figure 4). The location of the stations composing this cluster are scattered all across Europe, in
301 different climatic zones ranging from Continental to Mediterranean climate types (Figure 3). The
302 second-largest cluster, the winter cluster, contains 47 stations with a mean occurrence of no-flow
303 events between January and March (Figure 4). It includes stations with a snowmelt-driven annual
304 regime, such as the Pyrenees or Scandinavia, that experience cessation of flow due to freezing. The
305 fall cluster (29 stations) corresponds to late fall (November to January) occurrence of zero-flow
306 days. The main difference in flow regime for the fall and winter clusters is a more sustained runoff
307 rate during January-March for the fall cluster (Figure 4), indicating that zero-flow days for the
308 winter cluster are mostly due to freezing. As shown in this analysis, for most stations (Clusters 1
309 and 3), the zero-flow conditions are more frequently observed in summer months or during winter
310 or early spring due to snow and ice cover. Yet, as shown in the map in Figure 3, there are no clear

311 spatial patterns that could be identified from this analysis though the stations belonging to the
312 winter cluster are located predominantly in mountainous or northern areas.

313

314 **4.2 Trend analysis**

315

316 The trend detection and subsequent analyses have been performed only for the 254 rivers with at
317 least 10 years with a minimum of 5 consecutive zero-flow days. The first trend analysis has been
318 carried out on annual, winter and summer mean dates of zero-flow occurrence, with the $\bar{\theta}$ metric
319 (eq. 4) computed on an annual or seasonal basis. The results, in terms of significant trends, indicate
320 for most rivers located in southern Europe a trend towards earlier occurrence in zero-flow days,
321 mostly for the annual and summer timescales (Figure 5). For the river in the Baltic region, the trend
322 toward later occurrence in zero-flow days for the summer and annual periods can be observed.
323 Conversely, more contrasted trends patterns are detected for winter, with both positive and negative
324 trends in the mean date for stations. A significant trend towards a later occurrence of zero-flows is
325 visible in southern France and central Spain for the winter period.

326

327 The second trend analysis is concerning annual and seasonal sums and maximum lengths of zero-
328 flow days. It must be noted that the annual number of zero-flow days and the annual maximum
329 length of zero-flow periods are correlated, with an average correlation coefficient equal to 0.9 for
330 all stations. For the summer and winter, these correlations are lower and equal to 0.74 and 0.70,
331 respectively.

332 At the annual scale, 60 stations (24%) have positive trends in the number of zero-flow days and
333 more generally there are more positive trends detected by comparison to negative trends for all
334 indicators (Table 1 and Figure 6). Overall, the trends are very similar between the extreme duration
335 of zero-flow periods and the annual sum (Figure 7): on the 60 stations showing a decrease in annual
336 sum, 45 also have decreasing trends in the maximum duration of dry spells (similar behavior is
337 observed for positive trends). Since on average the trends affect about 30% of stations, these trends
338 (both positive and negative) are field-significant according to the FDR procedure. The trend
339 analysis results indicate that at the annual and seasonal timescales the majority of the detected
340 trends are towards an increase in dryness (in about 10% to 23% of stations as shown in Table 1).

341 At the seasonal timescale, there is a marked trend towards an increase in summer zero-flows, but

342 fewer trends detected for winter. When comparing trends at the annual and seasonal scales, in 60
343 stations with a significant increase of annual zero-flow days, 46 stations also have a significant
344 increase in summer zero-flow days. Conversely, a lower similarity between annual and winter
345 trends is observed. Thus, it can be concluded that the summer drying is the main driver for the
346 decreasing trends in the number of zero-flow days at the annual scale for these stations. Overall,
347 fewer trends are detected for extreme durations compared to annual or seasonal totals (Table 1),
348 with the notable exception of the winter maximum lengths of zero-flow days that are increasing in
349 the majority of stations. The results of the trend analysis have been compared with catchment sizes
350 but no relationship could be found between the trends in river intermittence and the size of the
351 basins considered.

352

353

354 **4.3 Links with SPEI anomalies**

355

356 In the first step, a trend analysis has been performed on SPEI over the different basins for different
357 aggregation periods 6, 12, 18 and 24 months. The results show a clear pattern with positive trends
358 at stations located north of 45°N and negative trends in the south. These trends have been
359 previously detected by Spinoni et al. (2017). At stations located north of 45N due to lower
360 temperature variability, the SPIE index responds mainly to the variability in precipitation. To check
361 if the SPEI anomalies could be explanatory covariates for the inter-annual variability of zero-flow
362 day occurrences, the SPEI with different aggregation time has been correlated with the number of
363 zero-flow days and the maximum dry spell lengths. Results show a strong association of zero-flow
364 days with SPEI anomalies in particular at the annual and summer timescales, with significant
365 correlations in more than half of the stations (Figure 8), with a lower number of significant
366 correlations during winter. The annual or seasonal sums of zero-flow days are more strongly
367 associated with SPEI anomalies than the maximum length of dry spells. The correlations are
368 negative for all SPEI timescales (Figure 9), indicating that negative SPEI anomalies, i.e.
369 pronounced net precipitation deficits, are linked with a larger number of zero-flow days. For about
370 one-third of stations (36%), there is no significant correlations. These stations are mostly located
371 in Spain, southern France, North Africa, Cyprus, but also Belgium, without a clear spatial pattern.
372 Therefore, a strong spatial variability of the spatial pattern is once again evident indicating local

373 influences on the relationship between zero-flow days and SPEI. The strength of the correlations
374 is higher for basins with a larger annual average number of zero-flow days for almost all SPEI
375 timescales. This demonstrates that strongly intermittent basins (i.e. basins with a large proportion
376 of zero-flow days) are more influenced by climatic variations to determine the annual number of
377 zero-flow days. This is probably due to the fact that these streams are often close to the wet/dry
378 threshold and consequently immediately impacted by a variation of precipitation availability. There
379 is also statistically a significant but moderate ($\rho=0.2$) correlation between the strength of the
380 correlations with the SPEI12 and basin size. This indicates that the influence of SPEI12 might be
381 stronger for smaller basins since larger basins are more likely to be more influenced by human
382 activities while small basins respond more quickly to precipitation and might have lower local
383 water storage capacity. Yet, this relationship is not significant for the SPEI18 and SPEI24. Smaller
384 basins have a reduced water storage capability in the context of climate variability so this behavior
385 is expected.

386

387 **4.3 Relations with large-scale atmospheric circulation**

388

389 As the large-scale climate drivers have a low-frequency time variability, the correlation analysis
390 should consider long time series. This is the reason why only rivers with at least 30 years of data
391 during 1970-2010 have been considered to analyze the relationships with large scale circulation
392 indices. The AMO and NAO indices are the most influential climate indices on zero-flow
393 occurrences. Since very low correlations were found with the other indices, we focus the analysis
394 of the results with AMO and NAO. At the annual scale, the AMO was the index with the highest
395 number of positive correlations, 21% for the longest annual no-flow event and 23% for the annual
396 sum. Results for both metrics in seasons are presented in Table 2. The summer and the winter AMO
397 are the drivers with the strongest links to the summer and winter metrics. A cluster of rivers
398 positively associated with the winter AMO is well recognizable in northern Europe (Norway,
399 Finland) for both winter metrics (Figure 10). Northern regions including the UK and south Sweden
400 exhibit a negative link between winter AMO and the winter sum of zero-flow days. A similar
401 pattern is observed for the summer with annual AMO. Additionally, the southern Mediterranean
402 part of Europe might be positively influenced by the summer AMO.

403

404 The conclusion can be drawn that the AMO is a potential driver of the intermittence in about 20%
405 of stations and its influence can be stretched to the following season. The associations with the
406 NAO are less frequent. However, the apparent cluster of rivers with a negative link to the winter
407 NAO can be observed in the Scandinavian Peninsula for both winter metrics (Figure 10). The rivers
408 positively linked to JJA NAO are scattered over Europe. It is worth emphasizing that this large-
409 scale climate effect can be hidden by more local climate conditions. The relationship between
410 climate drivers and hydrological characteristics in Europe has been previously documented by
411 many researchers (e.g., Valty et al. 2015, Wrzesiński & Paluszkiwicz 2011). Results of the present
412 analysis are to a large extent consistent with results obtained by Hurrell and Folland (2002),
413 Linderholm et al. (2009), Giuntoli et al. (2013) indicating that the NAO and AMO could influence
414 hydrological droughts.

415

416 **5. DISCUSSION AND CONCLUSIONS**

417

418 This study provides the first European-scale assessment of the trends in river intermittence over
419 the last decades. The most striking results are (i) the strong spatial variability of the detected trends,
420 and (ii) the seasonality and relationships with climate drivers. Overall, there is considerable spatial
421 variability of flow intermittence. Snelder et al. (2013) previously observed over France that the
422 high spatial heterogeneity in small-scale processes associated with intermittence partly explains
423 the low spatial synchronization of zero-flows. Significant trends are detected in about 30% of
424 stations, with most of detected trends towards an increasing number of zero-flow days, tending to
425 occur earlier in the season, in particular around the Mediterranean basin. For most basins, there is
426 a strong association of zero-flow days with SPEI negative anomalies, but neighbouring basins may
427 exhibit different relationships showing again the strong spatial variability. This indicates that the
428 SPEI could be a valid predictor for zero-flow occurrence, and the decreasing trend in this indicator
429 observed over southern Europe may explain the trends in flow intermittence obtained in this study.
430 Recent studies have shown that these downward trends in SPEI are mostly explained by an increase
431 in the atmospheric evaporative demand rather than a decline in precipitation (Vicente-Serrano et
432 al., 2020, Peña-Angulo et al., 2020). In a climate change context with increasing temperatures, it
433 is likely that this trend will continue in the future, with a possible increase in river intermittence
434 for these regions.

435
436 The strong spatial variability observed on trends in intermittence characteristics implies that
437 regional predictions or generalizations for flow intermittence patterns should be interpreted with
438 caution. Any mapping or extrapolation from such regional results may be prone to considerable
439 errors if not considering basin characteristics that are likely to play a strong role in determining
440 flow intermittence properties. In this study, the individual catchment characteristics (i.e.
441 topography, geology, land use, soil types) have not been analyzed, which would require a major
442 work at such a continental-wide scale. Catchment characteristics may be helpful to distinguish the
443 different patterns in flow intermittence since, as shown in this study, the geographical location or
444 basin sizes do not exert a strong control on river intermittence. In particular, it would be particularly
445 interesting to distinguish basins with strong surface-groundwater interactions that could explain
446 some of the patterns described in the present study. However, as noted by Snelder et al. (2013),
447 flow intermittence is also controlled by processes operating at scales smaller than catchments, thus
448 capturing these processes would require a much more detailed investigation than classical regional
449 approaches to take into account the local physiographic characteristics (Tramblay et al., 2010).

450
451 A major uncertainty of the present work and, to a greater extent, applicable to all ecohydrological
452 research on intermittent rivers is the definition of the zero-flow days and the lack of regional
453 representativeness of the monitoring networks. With regard to the first aspect, there is a wide
454 variety of measurements procedures in different European countries, leading to different accuracy
455 of the measured discharge values, in particular the minimal values. For example, in the UK or in
456 France the data is provided in $\text{m}^3.\text{s}^{-1}$ with an accuracy of three decimals, but for many other
457 countries, the minimum reported discharge is sometimes much greater than $1 \text{ L}.\text{s}^{-1}$ due to different
458 measuring methods. In addition, many rating curves at open channel stations have uncertainty at
459 low flows caused by instability of the riverbed. In the present work, we considered a strict criterion
460 to identify zero-flow days, but a more adequate selection could be made possible if good quality
461 metadata information were available for most rivers, which is not currently the case for several
462 countries. With regard to the second aspect of regional representativeness, several studies have
463 highlighted the lack of measurements for intermittent rivers (Skoulikidis et al., 2017, Costigan et
464 al., 2017). The number of monitored head water streams which are likely to be intermittent is indeed
465 much smaller than the number of perennial and large streams in national and international

466 databases, although their contribution to the water resources is probably high. This questions the
467 rationale behind national measurement strategies for intermittent streams, in particular, the most
468 ephemeral ones, since they may be overlooked in water resources management in comparison to
469 perennial streams. Depending on the national monitoring strategies of the river network, it is
470 possible that the selection of intermittent rivers to be monitored may be biased towards a specific
471 type of rivers within a given geographic location of geological properties.

472
473 Another important aspect to take into consideration is the regulation status of the monitored rivers,
474 which may evolve over time and not be available in the stations' metadata. In the present work, the
475 selected basins are those described as natural or weakly altered based on their metadata
476 information. Yet, how to quantitatively define "weakly altered" between different national
477 networks and monitoring protocols? This definition may differ from one country to another
478 without a common objective criterion to define the percentage of natural discharge being diverted
479 or used for water supply. Besides river alterations, often assumed to be an expert judgement, the
480 quantitative evaluation of the water uptake would require extensive work to monitor and collect
481 water consumption data over time. Even for a river considered to be unaltered, diffuse groundwater
482 pumping may occur and therefore have impacts on the groundwater-surface interactions, which
483 could in turn strongly impact intermittence occurrence. Two examples of the influence of river
484 status as described in the metadata on the trend results may be found in the UK. The Coal Burn
485 River is classified as broadly natural but is an experimental catchment set up to assess the impact
486 of afforestation and the trend analysis indicates an increase in zero-flow days, showing that the
487 influence of land-use change might indeed be significant on this aspect of the flow regime. The
488 limestone Slea River that conversely experienced a decrease in zero-flow days was also classified
489 as natural, but further scrutiny revealed a discharge augmentation scheme installed in 1995. Taking
490 into account all these local specificities in addition to the available metadata would require
491 tremendous effort and the information may not always be as readily available. The main findings
492 of the present study are an incentive to implement process-based studies on the intermittence
493 characteristics for different climatic and physiographic environments taking into account
494 watersheds characteristics.

495

496

497 **Acknowledgements**

498
499 This research is part of the COST action CA15113 SMIRES, Science and Management of
500 Intermittent Rivers and Ephemeral Streams <https://www.smires.eu/>, a short term scientific mission
501 has been funded for Agnieszka Rutkowska. Agnieszka Rutkowska was also supported by the
502 Ministry of Science and Higher Education of the Republic of Poland (grant DS 3371). The different
503 data providers are gratefully acknowledged. Some of the station data were retrieved from the
504 Global Runoff Data Centre (56068 Koblenz, Germany). The authors would like to thank two
505 anonymous reviewers, Kendra Keiser and the Associated Editor, Stephanie Kampf, for their
506 constructive comments.

507
508 **Data Availability Statement**

509
510 The different indices computed in the present work are made available to the community for
511 research applications upon request to the first author.

512
513 **References**

514
515 Beaufort, A., Carreau, J., Sauquet, E., 2019. A classification approach to reconstruct local daily
516 drying dynamics at headwater streams. *Hydrological Processes*, 33, 1896– 1912.

517
518 Beguería, S., Vicente-Serrano, S. M., Reig, F., Latorre, B., 2014. Standardized precipitation
519 evapotranspiration index SPEI revisited: parameter fitting, evapotranspiration models, tools,
520 datasets and drought monitoring. *International Journal of Climatology*, 34, 3001–3023.

521
522 Benjamini, Y., Hochberg, Y., 1995. Controlling the false discovery rate: A practical and powerful
523 approach to multiple testing. *Journal of the Royal Statistical Society, series B*, 57, 289–300.

524
525

526 Bormann, H., Pinter, N., 2017. Trends in low flows of German rivers since 1950: Comparability
527 of different low-flow indicators and their spatial patterns. *River Research and Applications*, 33,
528 1191– 1204.

529

530 Burn, D.H., 1997. Catchment similarity for regional flood frequency analysis using seasonality
531 measures. *Journal of Hydrology*, 202, 212-230.

532

533 Coch, A., Mediero, L., 2016. Trends in low flows in Spain in the period 1949–2009, *Hydrological*
534 *Sciences Journal*, 61:3, 568-584.

535

536 Costigan, K., Kennard M., Leigh C., Sauquet E., Datry T., Boulton A.J., 2017. Chapter 2.2 – Flow
537 regimes in intermittent rivers and ephemeral streams. In: “Datry T., Bonada N. & Boulton A.J.
538 Eds., *Intermittent Rivers and Ephemeral Streams. Ecology and Management*”, Academic Press pp.
539 51–78. doi: 10.1016/c2015-0-00459-2.

540

541 Datry, T., Singer, G., Sauquet, E., Jorda-Capdevilla, D., Von Schiller, D., Subbington, R., Magand,
542 C., Pařil, P., Miliša, M., Acuña, V., Alves, M., Augeard, B., Brunke, M., Cid, N., Csabai, Z.,
543 England, J., Froebrich, J., Koundouri, P., Lamouroux, N., Martí, E., Morais, M., Munné, A., Mutz,
544 M., Pesic, V., Previšić, A., Reynaud, A., Robinson, C., Sadler, J., Skoulikidis, N., Terrier, B.,
545 Tockner, K., Vesely, D., Zoppini, A., 2017. *Science and Management of Intermittent Rivers and*
546 *Ephemeral Streams SMIRES. Research Ideas and Outcomes* 3: e21774.
547 <https://doi.org/10.3897/rio.3.e21774>

548

549 D'Ambrosio, E., De Girolamo, A.M., Barca, E., Ielpo, P., Rulli, C., 2017.
550 Characterising the hydrological regime of an ungauged temporary river
551 system: a case study. *Environmental Science and Pollution Research*, 24,
552 13950–13966. doi:10.1007/s11356-016-7169-0

553

554 De Girolamo, A.M., Bouroui, F., Buffagni, A., Pappagallo, G., Lo Porto, A., 2017. Hydrology
555 under climate change in a temporary river system: Potential impact on water balance and flow
556 regime. *River Research and Applications*, 33, 1219-1232.

557
558 Delso, J., Magdaleno, F., Fernández-Yuste, J.A., 2017. Flow patterns in temporary rivers: a
559 methodological approach applied to southern Iberia. *Hydrological Sciences Journal*, 62:10, 1551-
560 1563,
561
562 Döll, P., & Schmied, H. M., 2012. How is the impact of climate change on river flow regimes
563 related to the impact on mean annual runoff? A global-scale analysis. *Environmental Research*
564 *Letters*, 7(1), 14037. <https://doi.org/10.1088/1748-9326/7/1/014037>
565
566 Dörflinger, G., 2016. A new spatial basis for rivers monitoring and management in Cyprus. DProf
567 thesis. Middlesex University. [online]. Available from: <http://eprints.mdx.ac.uk/20817/> [Accessed
568 January 15, 2020].
569
570 Eng, K., Wolock, D. M., Dettinger, M. D., 2016. Sensitivity of Intermittent Streams to Climate
571 Variations in the USA. *River Research and Applications*, 32, 885–895.
572
573 Gallart, F., Llorens, P., 2004. Observations on land cover changes and water resources in the
574 headwaters of the Ebro catchment, Iberian Peninsula. *Physics and Chemistry of the Earth*, parts
575 A/B/C, 2911-12, 769-773.
576
577 Gallart, F., Amaxidis, Y., Botti, P., Canè, G., Castillo, V., Chapman, P., ..., & Tournoud, M.G.,
578 2010. Investigating hydrological regimes and processes in a set of catchments with temporary
579 waters in Mediterranean Europe. *Hydrological Sciences Journal*, 53:3, 618-628.
580
581 Giuntoli I., Renard, B., Vidal, J.-P., Bard, A. 2013. Low flows in France and their relationship to
582 large scale climate indices. *Journal of Hydrology*, 482, 105–118
583
584 Gustard, A., Bullock, A., Dixon, J.M., 1992. Low flow estimation in the United Kingdom. Report
585 N°108, Institute of Hydrology, Wallingford, UK. 292p.
586

587 Hamed, K. H. Rao, A. R., 1998. A modified Mann-Kendall trend test for autocorrelated data,
588 Journal of Hydrology, 204, 182–196.

589

590 Hannaford, J., Lloyd-Hughes, B., Keef, C., Parry, S., Prudhomme, C., 2011. Examining the large-
591 scale spatial coherence of European drought using regional indicators of precipitation and
592 streamflow deficit. Hydrological Processes, 25: 1146–1162.

593

594 Hertig, E., Trambly, Y., 2017. Regional downscaling of Mediterranean droughts under past and
595 future climatic conditions. Global and Planetary Change, 151, 36-48.

596

597 Hurrell, J.W., Folland, C.K., 2002. The relationship between tropical Atlantic rainfall and the
598 summer circulation over the North Atlantic. CLIVAR Exchanges, 25, 52–54

599

600 Ionita, M., Tallaksen, L. M., Kingston, D. G., Stagge, J. H., Laaha, G., Van Lanen, H. A. J., Scholz,
601 P., Chelcea, S. M., Haslinger, K., 2017. The European 2015 drought from a climatological
602 perspective. Hydrology and Earth System Sciences, 21, 1397-1419.

603

604 Kennard, M.J., Pusey, B.J. Olden, J.D., Mackay, S.J., Stein, J.L., Marsh, N., 2010. Classification
605 of natural flow regimes in Australia to support environmental flow management. Freshwater
606 Biology, 55, 171–193.

607

608 Kirkby, M. J., Gallart, F., Kjeldsen, T. R., Irvine, B. J., Froebrich, J., Porto, A. L., Girolamo, A.
609 D., 2011. Classifying low flow hydrological regimes at a regional scale. Hydrology and Earth
610 System Sciences, 1512, 3741-3750.

611

612

613 Laaha, G. & Blöschl, G., 2006. Seasonality indices for regionalizing low flows, Hydrol. Process.,
614 20,3851–3878.

615

616 Laaha, G., Gauster, T., Tallaksen, L. M., Vidal, J.-P., Stahl, K., Prudhomme, C., Heudorfer, B.,
617 Vlnas, R., Ionita, M., Van Lanen, H. A. J., Adler, M.-J., Caillouet, L., Delus, C., Fendekova, M.,

618 Gailliez, S., Hannaford, J., Kingston, D., Van Loon, A. F., Mediero, L., Osuch, M., Romanowicz,
619 R., Sauquet, E., Stagge, J. H., Wong, W. K., 2017. The European 2015 drought from a hydrological
620 perspective. *Hydrology and Earth System Sciences*, 21, 3001-3024.

621

622 Linderholm, H. W., Folland, C. K., Walther, A., 2009. A multicentury perspective on the summer
623 North Atlantic Oscillation SNAO and drought in the eastern Atlantic Region. *Journal of Quaternary*
624 *Science*, 24, 415–425.

625

626 Mann, H. B., 1945. Nonparametric tests against trend. *Econometrica*, 13,245– 259.

627

628 Marx, A., Kumar, R., Thober, S., Rakovec, O., Wanders, N., Zink, M., Wood, E.F., Pan, M.,
629 Sheffield, J., Samaniego, L., 2018. Climate change alters low flows in Europe under global
630 warming of 1.5, 2, and 3 °C. *Hydrol. Earth Syst. Sci.* 22, 1017–1032. [https://doi.org/10.5194/hess-](https://doi.org/10.5194/hess-22-1017-2018)
631 [22-1017-2018](https://doi.org/10.5194/hess-22-1017-2018)

632 McKee, T. B., Doesken, N.J., Kleist, J., 1993. The relationship of drought frequency and duration
633 to time scales. Preprints, Eighth Conf. on Applied Climatology. Anaheim, CA, Amer. Meteor. Soc.,
634 179–184.

635

636 Myronidis, D., Ioannou, K., Fotakis, D., Dörflinger, G., 2018. Streamflow and Hydrological
637 Drought Trend Analysis and Forecasting in Cyprus. *Water Resources Management*, 32, 1–18.

638 Osuch, M., Romanowicz, R.J., Wong, W.K., 2018. Analysis of low flow indices under varying
639 climatic conditions in Poland. *Hydrology Research*, 49 2: 373–389.

640 Oueslati, O., De Girolamo, A. M., Abouabdillah, A., Kjeldsen, T. R., Lo Porto, A., 2015.
641 Classifying the flow regimes of Mediterranean streams using multivariate analysis. *Hydrological*
642 *Processes*, 29: 4666–4682.

643

644 Peña-Angulo, D., Vicente-Serrano, S.M., Domínguez-Castro, F., González-Hidalgo, J.C., Murphy,
645 C., Hannaford, J., Reig, F., Tramblay, Y., Trigo, R.M., Luna, M.Y., Turco, M., Noguera, I.,
646 Aznarez, M., El Kenawy, A., García-Herrera, R., Tomas-Burguera, M., 2020. Precipitation in

647 Southwest Europe does not show clear trend attributable to anthropogenic forcing. *Environmental*
648 *Research Letters*, <https://doi.org/10.1088/1748-9326/ab9c4f>
649

650 Perez-Saez, J., Mande, T., Larsen, J., Ceperley, N., Rinaldo, A., 2017. Classification and prediction
651 of river network ephemerality and its relevance for waterborne disease epidemiology. *Advances in*
652 *Water Resources*, 110, 263-278.
653

654 Pournasiri Poshtiri, M., Pal, I., Lall, U., Naveau, P., Towler, E., 2019. Variability patterns of the
655 annual frequency and timing of low streamflow days across the United States and their linkage to
656 regional and large-scale climate. *Hydrological Processes*, 33, 1569– 1578.
657

658 Skoulikidis, N.T., Sabater, S., Datry, T., Morais, M.M., Buffagni, A., Dörflinger, G., ..., &
659 Tockner, C., 2017. Non-perennial Mediterranean rivers in Europe: Status, pressures, and
660 challenges for research and management. *Science of the Total Environment*, 577, 1–18.
661

662 Snelder, T. H., Datry, T., Lamouroux, N., Larned, S. T., Sauquet, E., Pella, H., Catalogne, C., 2013.
663 Regionalization of patterns of flow intermittence from gauging station records, *Hydrology and*
664 *Earth System Sciences*, 17, 2685-2699.
665

666 Stahl K., & Demuth S., 1999. Linking streamflow drought to the occurrence of atmospheric
667 circulation patterns. *Hydrological Sciences Journal*, 44, 467-482.
668

669 Stahl, K., Hisdal, H., Hannaford, J., Tallaksen, L. M., van Lanen, H. A. J., Sauquet, E., Demuth,
670 S., Fendekova, M., Jódar, J., 2010. Streamflow trends in Europe: evidence from a dataset of near-
671 natural catchments. *Hydrology and Earth System Sciences*, 14, 2367-2382.
672

673 Spinoni, J., Naumann, G., Vogt, J.J., 2017. Pan-European seasonal trends and recent changes of
674 drought frequency and severity. *Global and Planetary Changes*, 148, 113-130.
675

676 Tzoraki, O., De Girolamo, A.M., Gamvroudis, Ch., Skoulidakis, N., 2016. Assessing the Flow
677 alteration of temporary streams under current conditions and changing climate by SWAT model.
678 International Journal of River Basin Management, 14, 1571-5124.

679

680 Trambly, Y., St-Hilaire, A., Ouarda, T., Moatar, F., Hecht, B., 2010. Estimation of local extreme
681 suspended sediment concentrations in California Rivers. Science of the total environment, 408,
682 4221-4229.

683

684 Valty, P., de Viron, O., Panet, I., Collilieux, X., 2015. Impact of the North Atlantic Oscillation on
685 Southern Europe Water Distribution: Insights from Geodetic Data. Earth Interactions, 19, DOI:
686 10.1175/EI-D-14-0028.1.

687

688 Vicente-Serrano, S.M., Beguería, S., Lopez-Moreno, J.I., 2010. A multiscalar drought index
689 sensitive to global warming: the standardized precipitation evapotranspiration index – SPEI.
690 Journal of Climate, 23, 1696–1718.

691

692 Vicente-Serrano, S.M., Domínguez-Castro, F., Murphy, C., Hannaford, J., Reig, F., Peña-Angulo,
693 D., Trambly, Y., Trigo, R., MacDonald, N., Luna, Y., Guijarro, J.A., McCarthy, M., Van der
694 Schrier, G., Turco, M., Camuffo, D., Noguera, I., El Kenawy, A., García-Herrera, R., 2020. Long-
695 term variability and trends in meteorological droughts in Europe (1851-2018), International Journal
696 of Climatology, <https://doi.org/10.1002/joc.6719>

697

698 Ward, J. H., 1963. Hierarchical Grouping to Optimize an Objective Function. Journal of the
699 American Statistical Association, 58, 236–244.

700

701 Wilks, D.S., 2016. The stippling shows statistically significant grid points: how research results
702 are routinely overstated and overinterpreted, and what to do about it. Bulletin of the American
703 Meteorological Society, 97, 2263–2273.

704

705 Wrzesiński, D, & Paluszkiwicz, R., 2011. Spatial differences in the impact of the North Atlantic
706 Oscillation on the flow of rivers in Europe. Hydrology Research, 42, 30-39.

707
708 Zimmer, M. A., Kaiser, K. E., Blaszcak, J. R., Zipper, S. C., Hammond, J. C., Fritz, K. M.,
709 Costigan, K. H., Hosen, J., Godsey, S. E., Allen, G. H., Kampf, S., Burrows, R. M., Krabbenhoft,
710 C. A., Dodds, W., Hale, R., Olden, J. D., Shanafield, M., DelVecchia, A. G., Ward, A. S., Mims,
711 M. C., Datry, T., Bogan, M. T., Boersma, K. S., Busch, M. H., Jones, C. N., Burgin, A. J., and
712 Allen, D. C., 2020. Zero or not? Causes and consequences of zero-flow stream gage readings.
713 WIREs Water, Wiley, 7. <https://doi.org/10.1002/wat2.1436>.

714
715
716
717
718
719
720
721
722
723
724
725
726
727
728
729
730
731
732
733
734
735
736
737

738
739
740
741
742
743
744
745
746
747

TABLES

Table 1: Summary of the detected trends in the annual and seasonal number of zero-flow days and the maximum length of dry spells

| Variable | Positive trends | Negative trends | No trends |
|----------------|-----------------|-----------------|-----------|
| Annual sum | 23,62% | 10,24% | 66,14% |
| Annual maximum | 20,08% | 8,66% | 71,26% |
| Winter sum | 10,63% | 8,66% | 80,71% |
| Winter maximum | 23,23% | 9,45% | 67,32% |
| Summer sum | 23,62% | 6,69% | 69,69% |
| Summer maximum | 18,11% | 9,45% | 72,44% |

748
749
750
751
752
753

Table 2: Summary of catchments with significant correlations ($\alpha = 0.05$) between seasonal metrics of intermittence and large-scale climate drivers. The subscripts *s, w*, DJF, JJA, *w1* refer to the summer (Apr-Sep), winter (Sep-Mar), Dec-Feb, Jun-Aug, and winter from the preceding year, respectively.

| a) | Positive correlations | | Negative correlations | b) | Positive correlations | | |
|------------|-----------------------|------------------|-----------------------|------------|-----------------------|------------------|-------------------|
| Variable | AMO _s | AMO _w | NAO _{DJF} | Variable | NAO _{JJA} | AMO _s | AMO _{w1} |
| Winter max | 18% | 16% | 11% | Summer max | 11% | 21% | 18% |
| Winter sum | 21% | 19% | 11% | Summer sum | 9% | 22% | 21% |

754
755
756
757
758

759
760
761
762
763
764
765
766
767
768
769
770
771
772
773
774
775
776
777
778
779
780
781
782
783
784
785
786
787
788
789

FIGURES CAPTIONS

Figure 1: Number of stations having less than 5% missing data each year (left) and catchment sizes (right)

Figure 2: Mean annual percentage of zero-flow days for hydrological years

Figure 3: Cluster analysis on zero-flow seasonality. Colors represent seasonality of zero-flow events classified in three clusters (winter, summer, fall clusters).

Figure 4: Flow regime (left) and mean occurrence of zero-flow days (right) for the three clusters identified in figure 3.

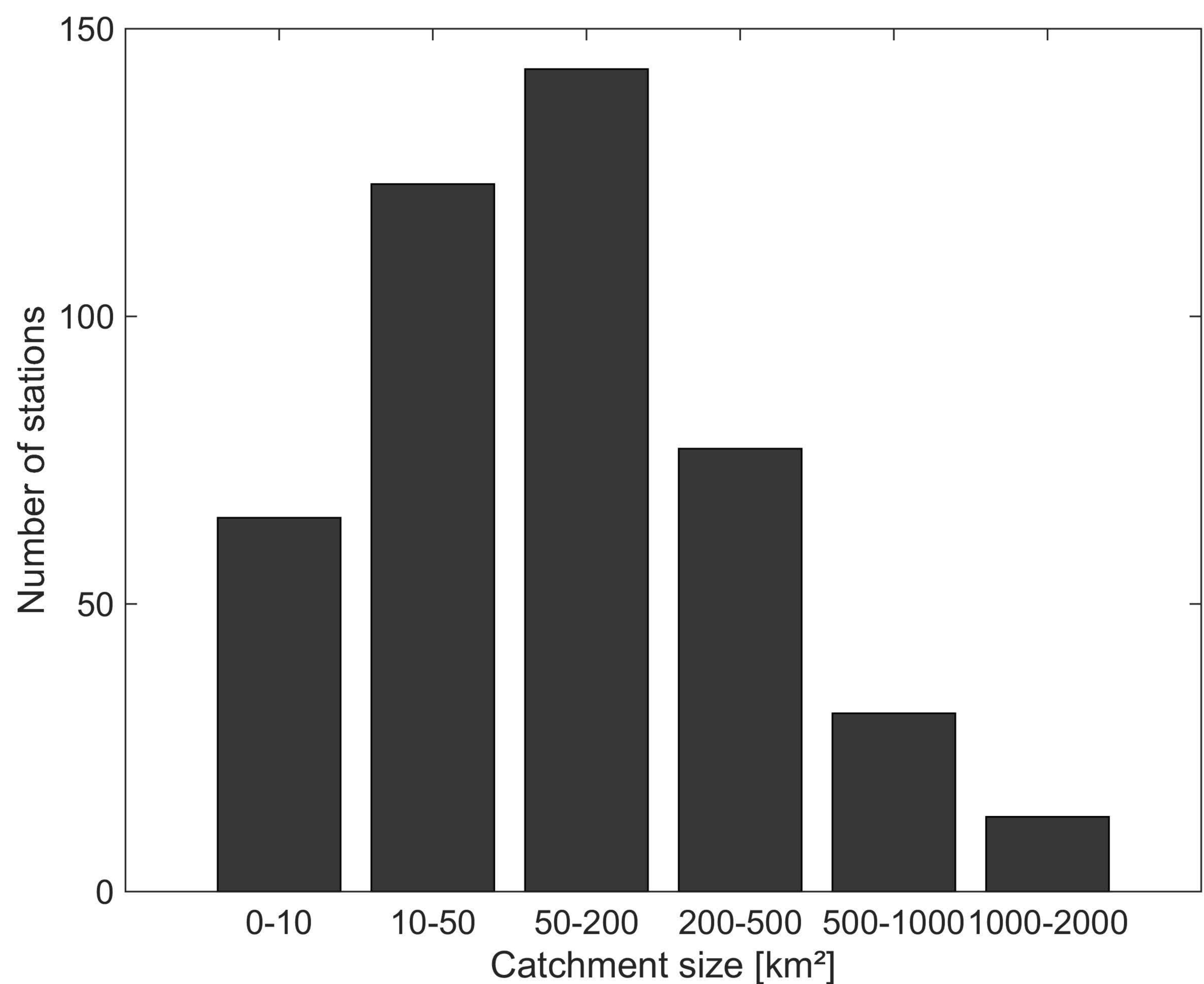
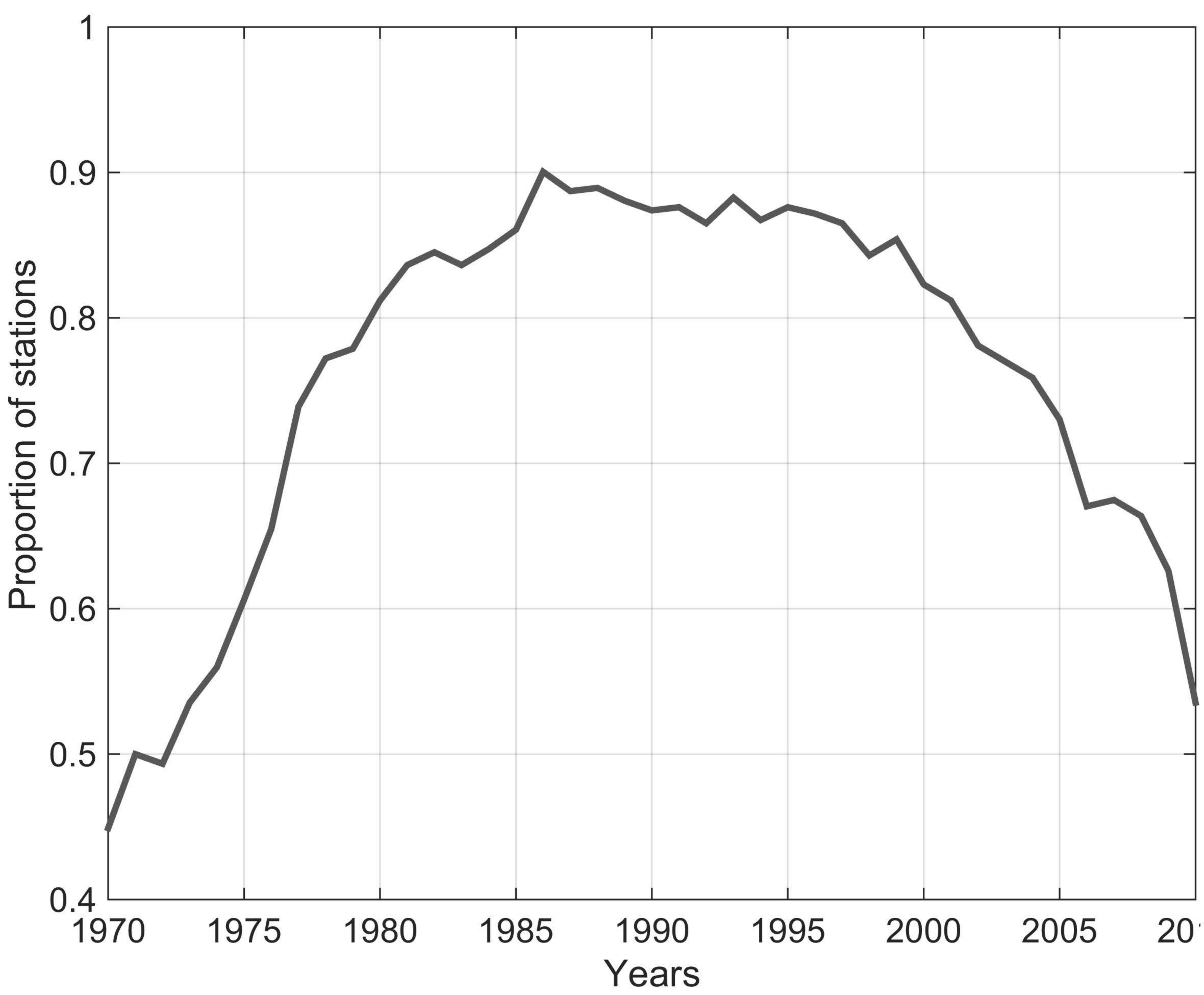
Figure 5: Significant increasing (later date) or decreasing (earlier date) trends in the mean date of zero-flow day occurrence, at the 10% significance level.

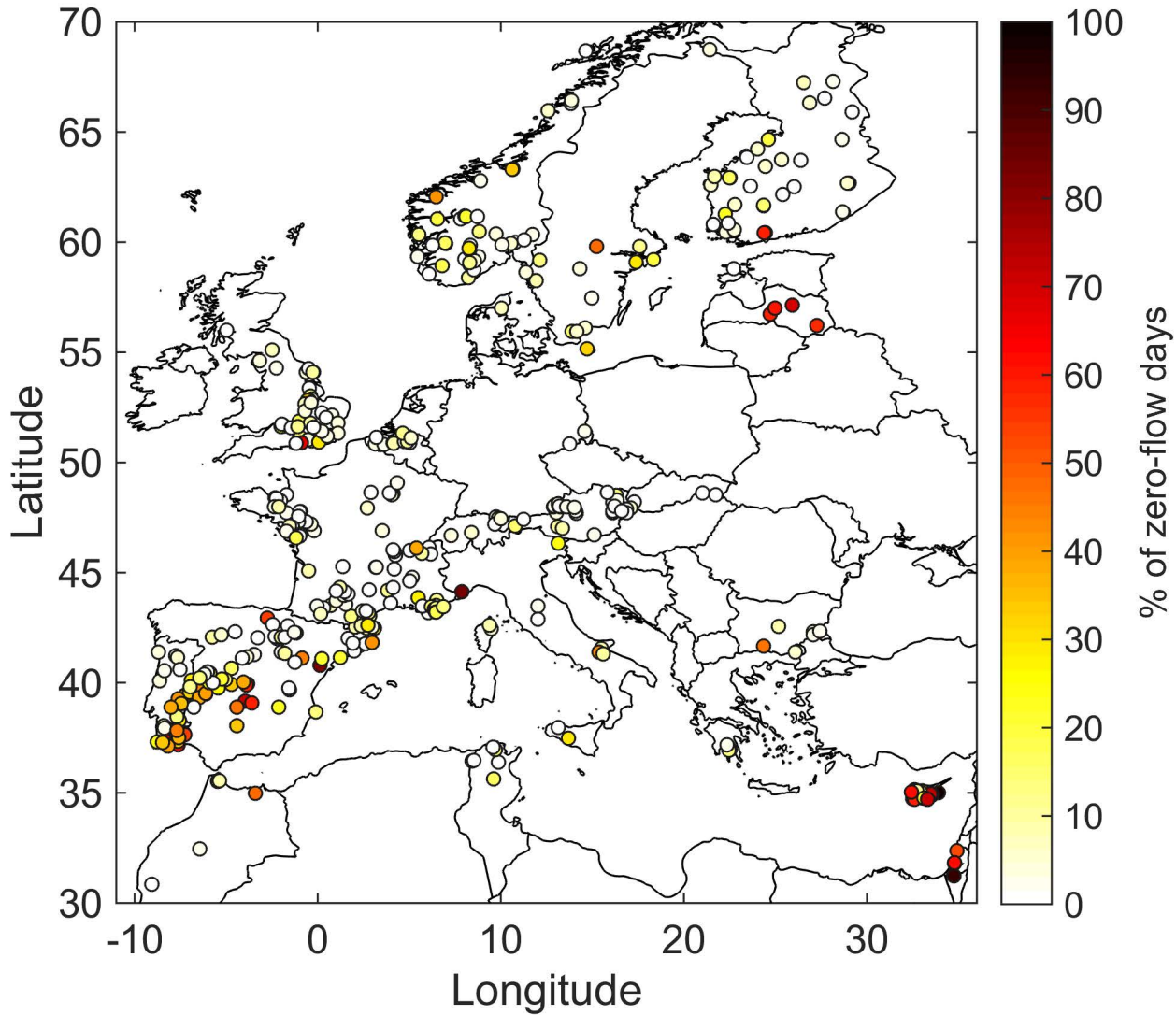
Figure 6: Increasing (red triangle up) or decreasing (blue triangle down) trends, at the 10% significance level, for the annual or seasonal mean number of zero flow days (left), the annual or seasonal maximum length of dry spells (right). On average for all indicators and seasons, 28% of stations have significant trends.

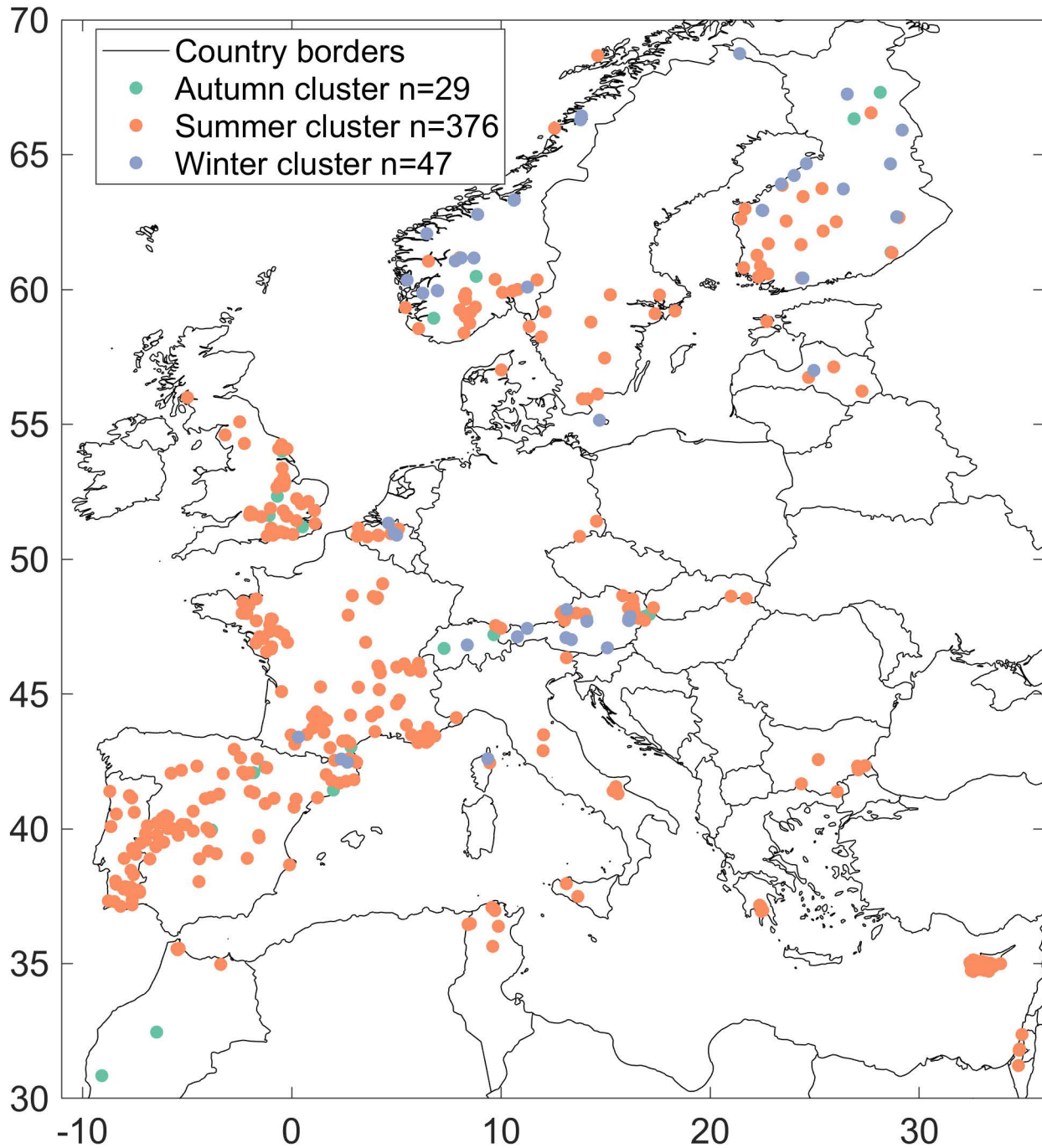
Figure 7: Scatter plot of the relationship between the Sen slope of trends in the annual number of zero-flow days and the annual maximum duration of zero-flow periods.

Figure 8: Significant correlations at the 5% level between annual, summer and winter sum of zero flow days, and the maximum length of dry periods with SPEI6, SPEI12, SPEI18 and SPEI24.

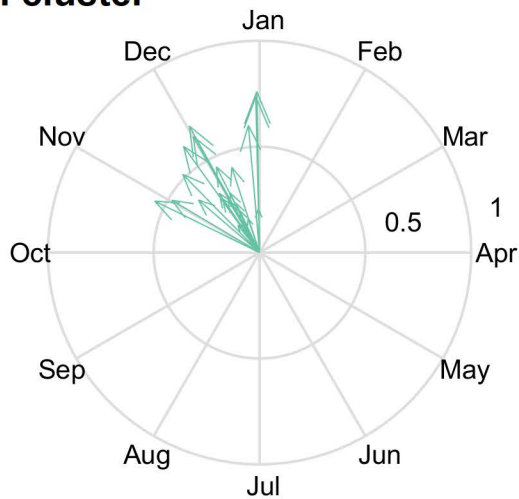
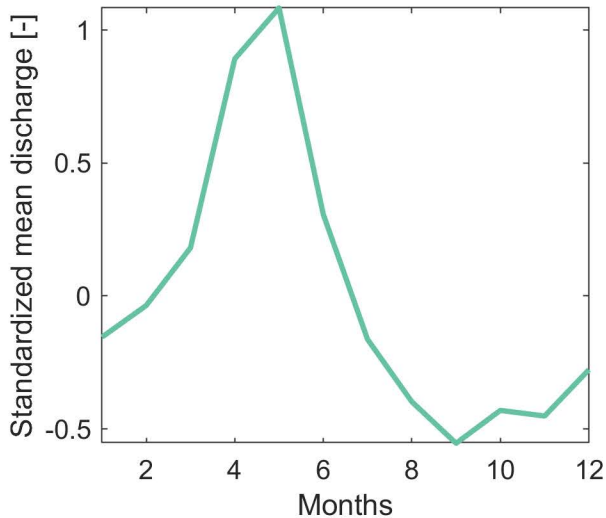
790 Figure 9: Map of the significant correlations between the annual sum of zero flow days (top) and
791 the annual maximum length of zero flow days (bottom) with the SPEI18. The black crosses
792 indicate stations where the correlation is not significant at the 10% level. Correlations are
793 negative because the smaller the SPEI (water deficit), the larger the number of zero-flow days.
794
795 Figure 10: Significant correlations between summer zero-flow days and AMO (left) and between
796 winter zero-flow days and NAO (right).



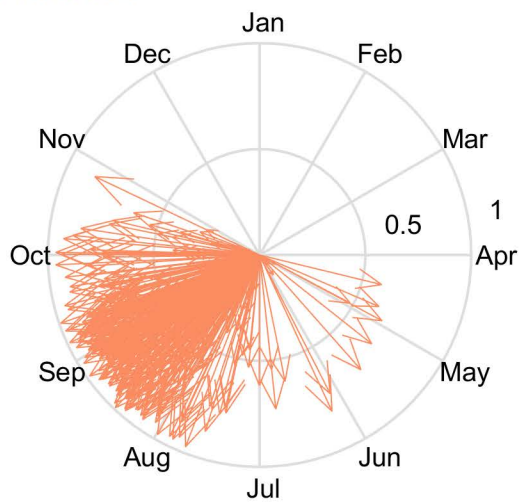
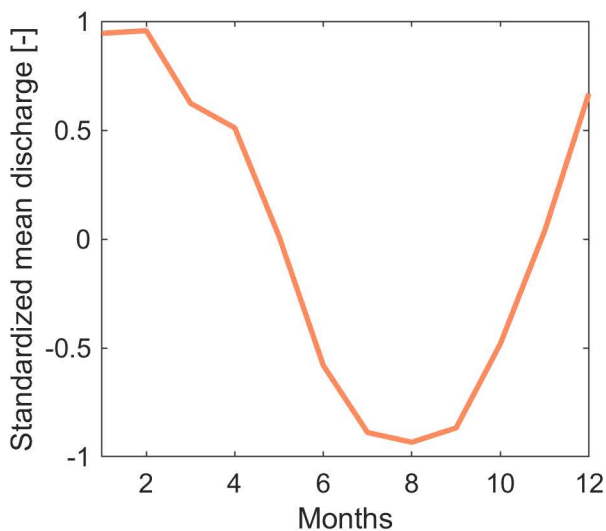




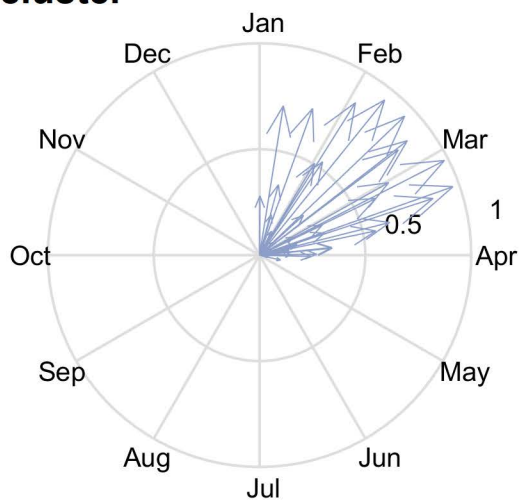
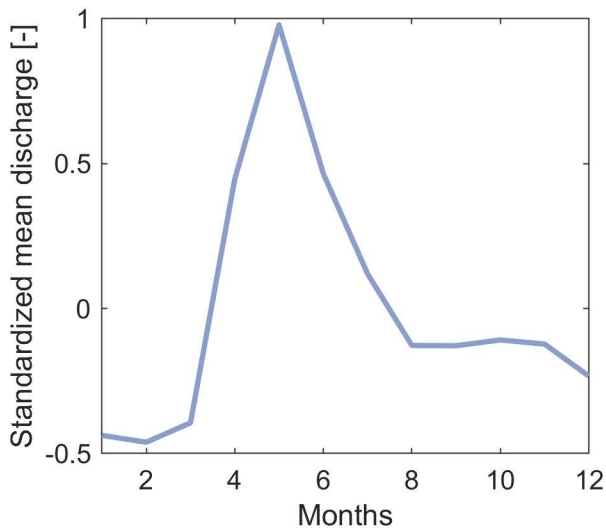
Autumn cluster



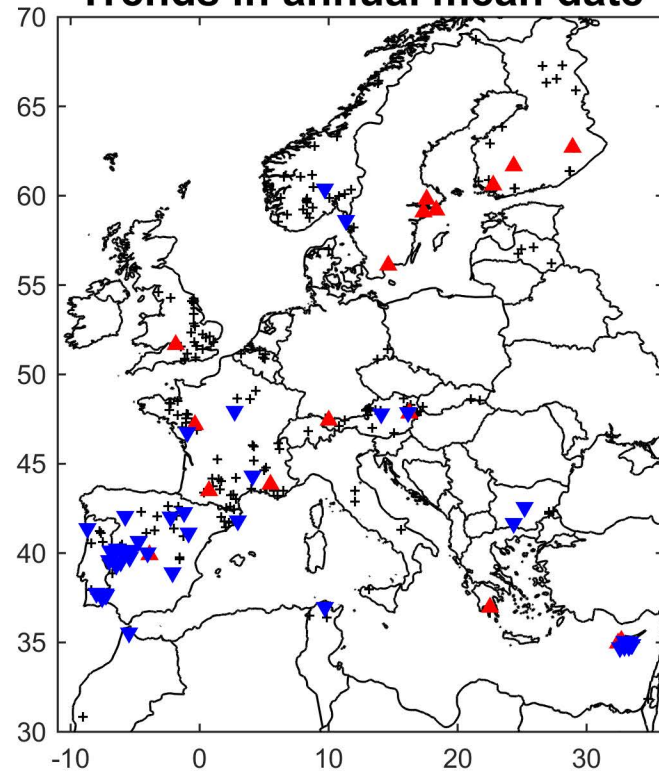
Summer cluster



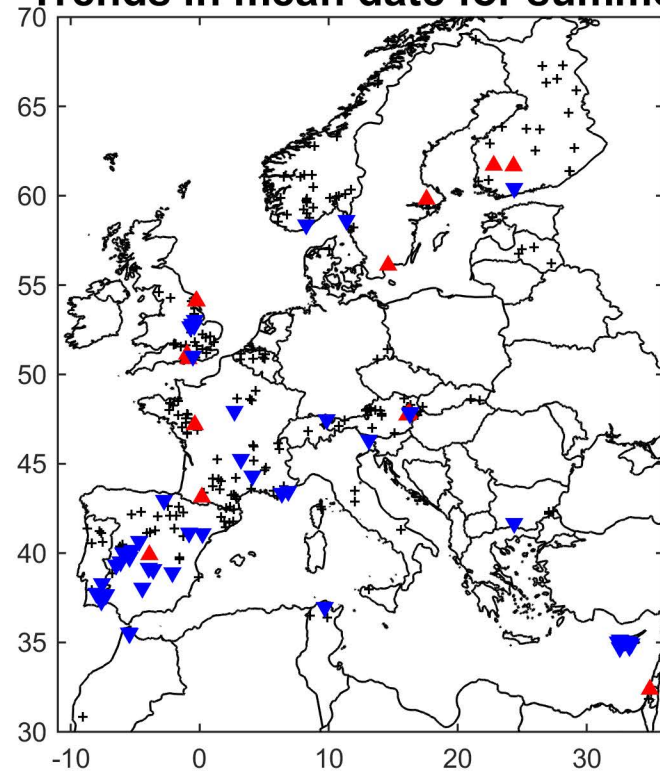
Winter cluster



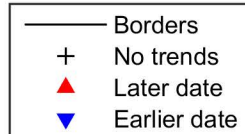
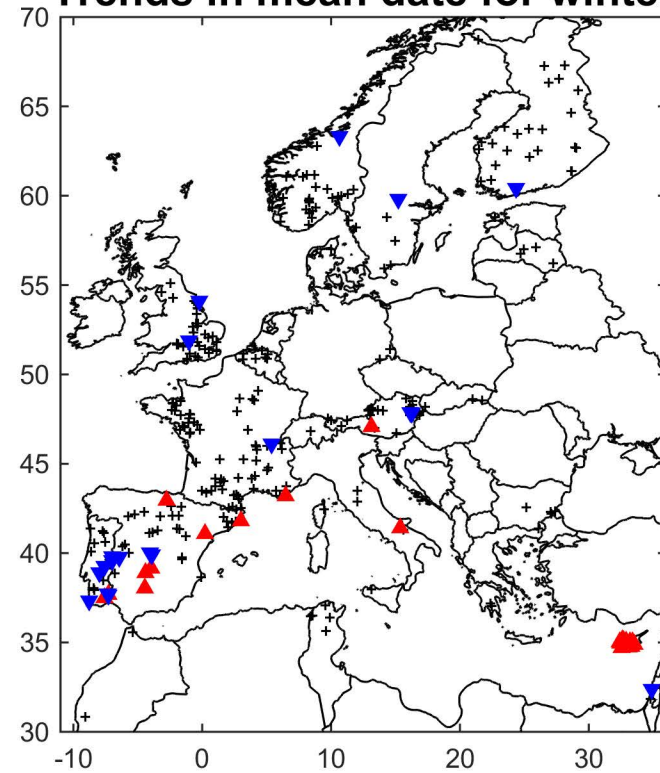
Trends in annual mean date



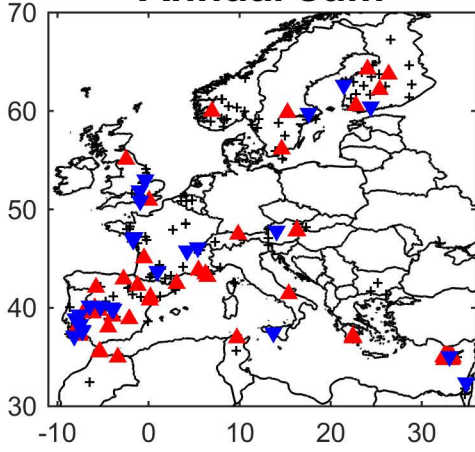
Trends in mean date for summer



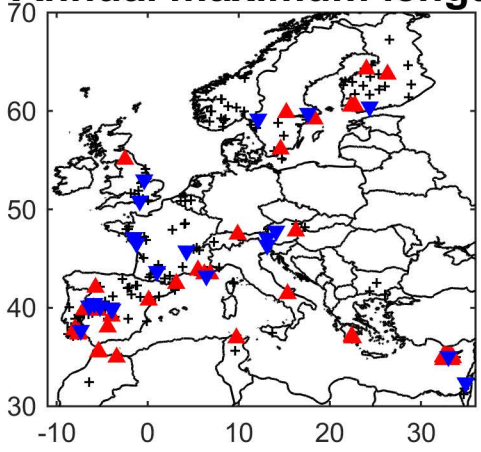
Trends in mean date for winter



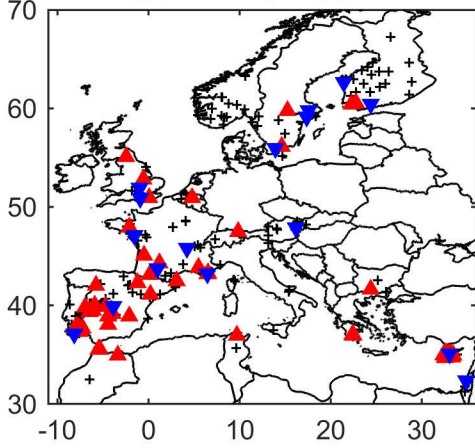
Annual sum



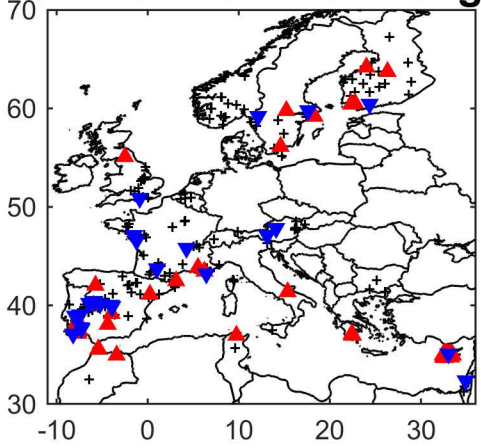
Annual maximum length



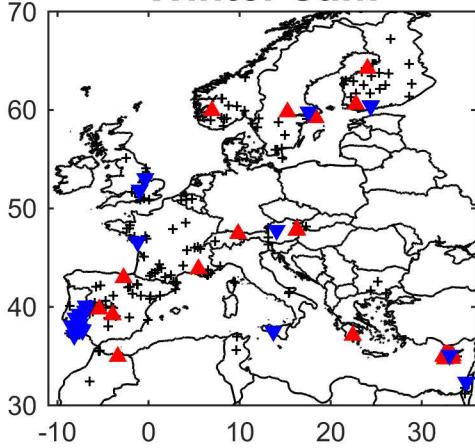
Summer sum



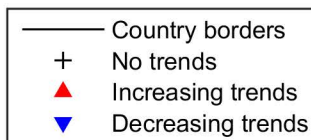
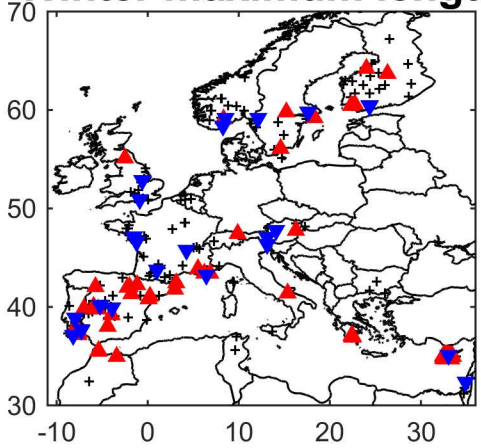
Summer maximum length



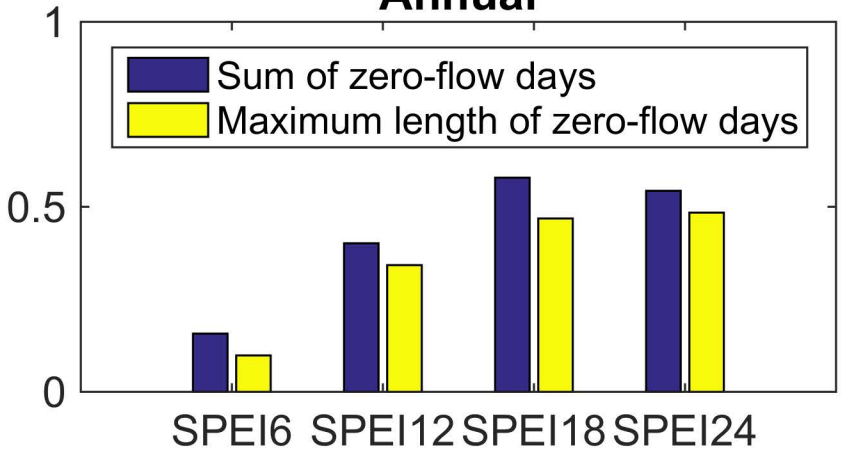
Winter sum



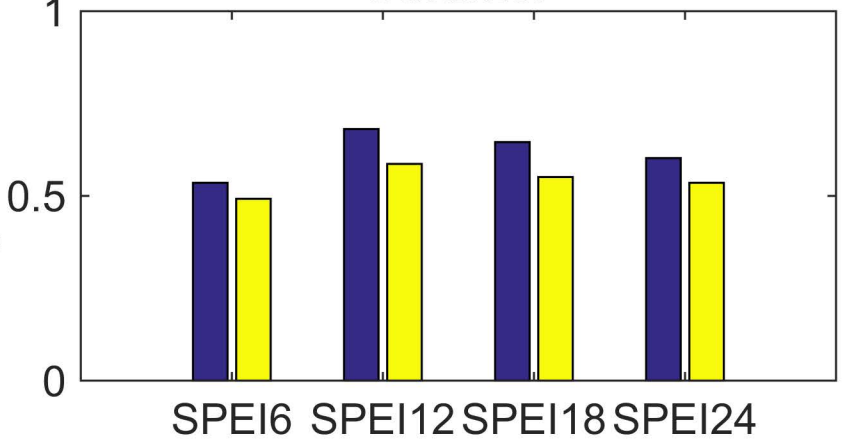
Winter maximum length



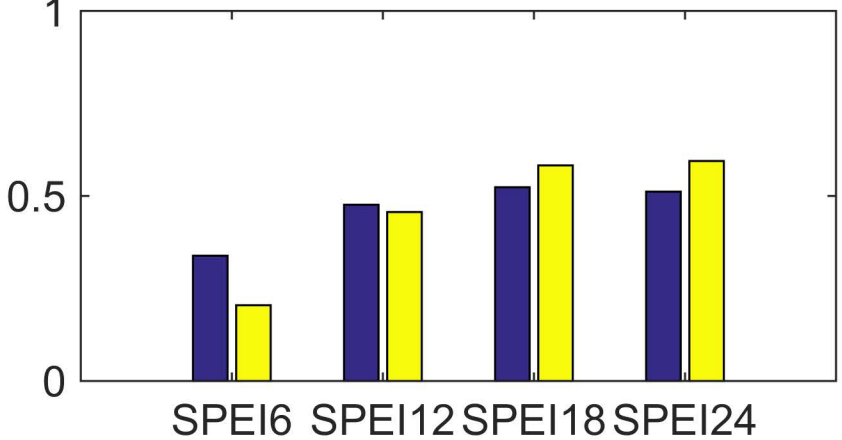
Annual



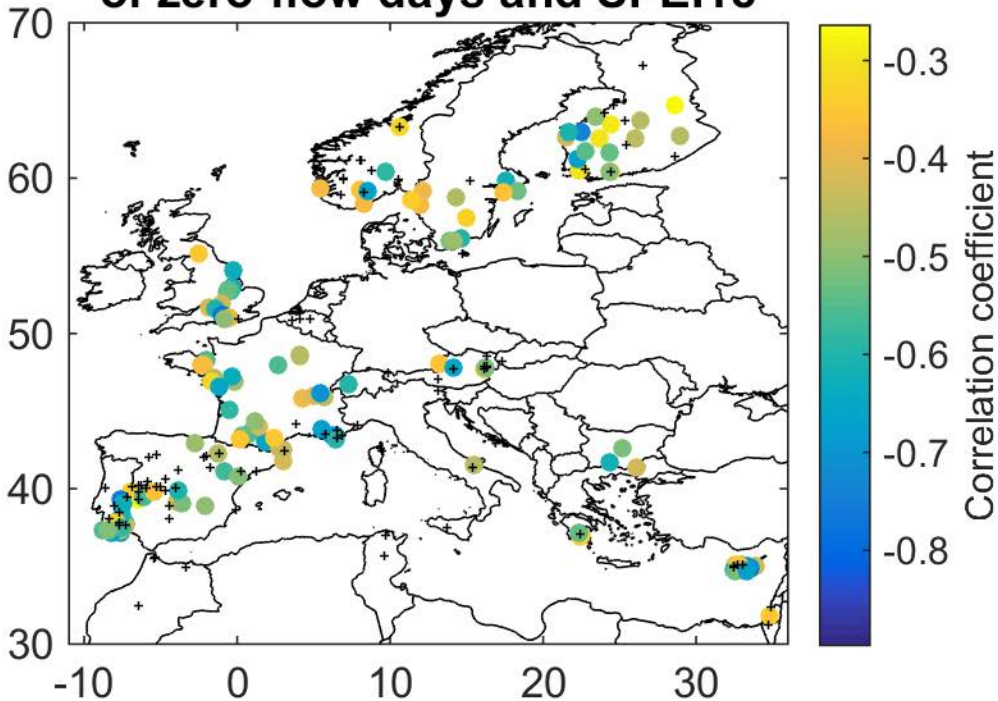
Summer



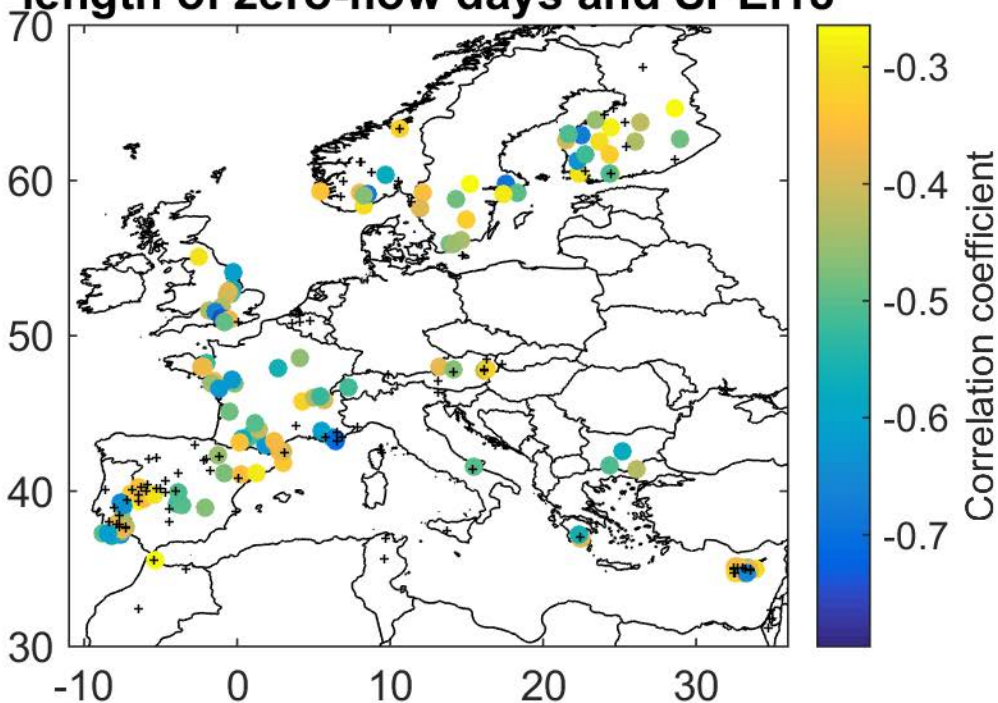
Winter



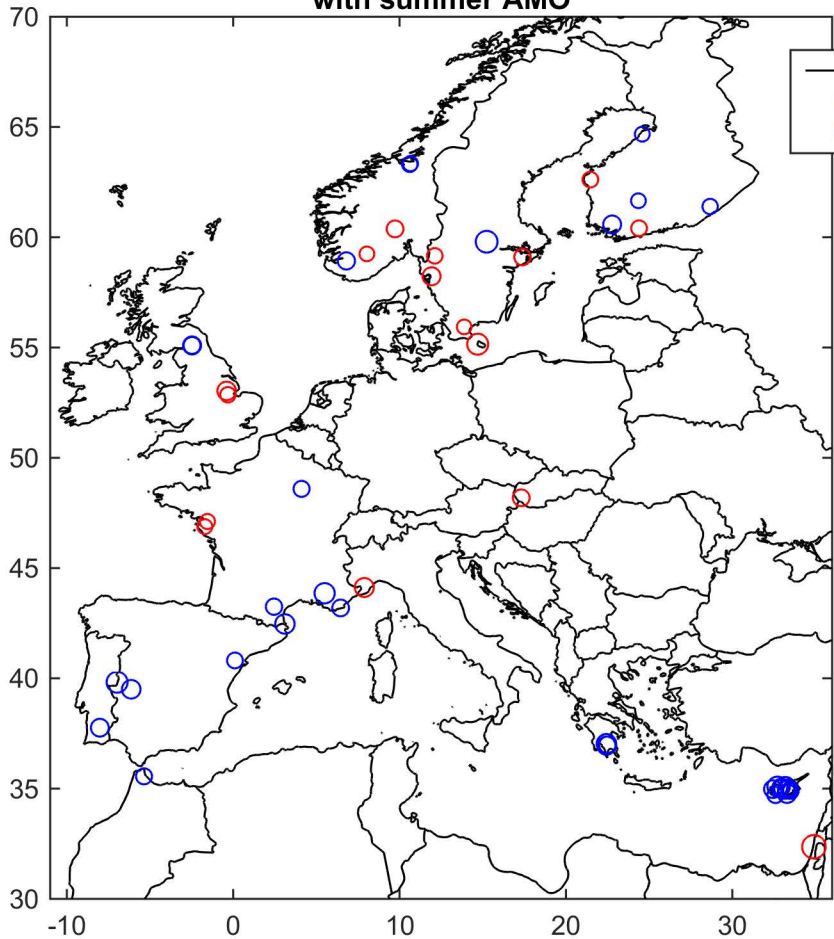
Correlation between annual sum of zero-flow days and SPEI18



Correlation between annual maximum length of zero-flow days and SPEI18



Correlation of summer sum of zeroflow days with summer AMO



Correlation of winter sum of zeroflow days with DJF NAO

